Biochemistry and Biophysics Reports 33 (2023) 101418

Contents lists available at ScienceDirect

Biochemistry and Biophysics Reports

journal homepage: www.elsevier.com/locate/bbrep

Acetylation of the nuclear localization signal in Ku70 diminishes the interaction with importin-α

Hirofumi Fujimoto [a,*], Togo Ikuta [b], Aki Koike [c], Manabu Koike [c,**]

[a] Department of Quality Assurance, Radiation Safety, and Information Management, National Institute of Infectious Diseases, Toyama 1-23-1, Shinjuku-ku, Tokyo, 162-8640, Japan
[b] Department of Cancer Prevention, Research Institute for Clinical Oncology, Saitama Cancer Center, Komuro 818, Ina-machi, Kitaadachi-gun, Saitama, 362-0806, Japan
[c] Institute for Quantum Medical Science, National Institutes for Quantum Science and Technology, Anagawa 4-9-1, Inage-ku, Chiba, 263-8555, Japan

A B S T R A C T

Proteins are functionally regulated by various types of posttranslational modifications (PTMs). Ku, a heterodimer complex of Ku70 and Ku80 subunits, participates in DNA repair processes. Ku is distributed not only in the nucleus but also in the cytoplasm, suggesting that the function of Ku is regulated by its subcellular localization. Although Ku70 undergoes PTMs including phosphorylation or acetylation, it remains unknown whether the PTMs of Ku70 affect the subcellular localization of Ku. Using a cell-free pull-down assay technique, we show that Nε-acetylation of lysine residues in the synthetic peptide matched to Ku70's nuclear localization signal (NLS) reduces the peptide's interaction with the nuclear transport factor importin-α. The reduced interaction by acetylation was supported by molecular simulation analysis. In addition, when expressed in the endogenous Ku80-defective Chinese hamster ovary xrs-6 cells, some full-size human Ku70 mutants with substitutions of glutamine, a possible structural mimetic of *N*ε-acetyl–lysine, for lysine at the specific NLS positions exhibited no nuclear distribution. These findings imply that acetylation of particular lysine residues in the Ku70 NLS regulates nuclear localization of Ku.

1. Introduction

A precise control mechanism of subcellular localization is essential for intracellular proteins, especially those that have functions in both the nucleus and the cytoplasm of a cell, such as many transcription factors or DNA repair proteins [1,2]. Ku70 is a subunit of Ku that forms Ku heterodimers with its homologous protein, Ku80. Ku has been well characterized as a DNA double-strand-break (DSB) sensor in the process of non-homologous end-joining, which is a major pathway for the repair of DSBs [3,4]. Because Ku70 and Ku80 coexist in the cytoplasm and their heterodimers have been discovered at least in the cytoplasm of HeLa cells during the mitotic phase, Ku heterodimers may develop in the cytoplasm [5]. On the other hand, it was reported that the cytoplasmic distribution of Ku70 is significantly higher than that of Ku80 in HeLa cells [6], suggesting that Ku70 and Ku80 can function separately in the cytoplasm [6–8]. We previously discovered that the nuclear localization signal (NLS) of human Ku70 is located between residues K539 and K556, the NLS is bound and transported to the nuclear rim by the nuclear transport factors importin-α/importin-β complexes (Impα/Impβ) [9], and the translocation of Ku70 from the cytoplasm to the nucleus is inhibited when lysine residues in the NLS region are replaced with alanine [10,11]. The NLS of Ku70 was thought to be classified as a bipartite NLS [12,13], and the molecular structure of the Ku70 NLS–Impα complex solved by X-ray crystallographic analyses revealed that the C-terminal of Ku70 NLS (N547 to K556) fit into the interaction site of Impα [14]. These findings indicate that Ku70 is translocated to the nucleus via the classical Impα/Impβ-mediated nuclear import pathway. In addition, the Ku70 NLS contains five lysine residues (K539, K542, K544, K553, and K556) that were identified as targets for acetylation *in vivo* [6,9]. Acetylation is a major protein posttranslational modification (PTM) that is thought to promote conformational changes that control association with or dissociation from other biomolecules by neutralizing positive charges [15]. However, whether the acetylation of the five lysine residues in the Ku70 NLS functions as a switch governing Ku70 translocation from the cytoplasm to the nucleus remains unknown. Here we demonstrate that the acetylation of lysine residues in the Ku70 NLS reduces the interaction with Impα using both experimental and theoretical approaches, and that recombinant Ku70 mutants in which specific NLS lysine residues were substituted with the uncharged amino acid glutamine exhibited reduced translocation to the nucleus. These findings imply that acetylation of certain lysine residues in the NLS regulates Ku70 translocation to the nucleus.

* Corresponding author.
** Corresponding author.
E-mail addresses: fuj@nih.go.jp (H. Fujimoto), togo@saitama-pho.jp (T. Ikuta), koike.aki@qst.go.jp (A. Koike), koike.manabu@qst.go.jp (M. Koike).

https://doi.org/10.1016/j.bbrep.2022.101418
Received 14 September 2022; Received in revised form 19 December 2022; Accepted 22 December 2022

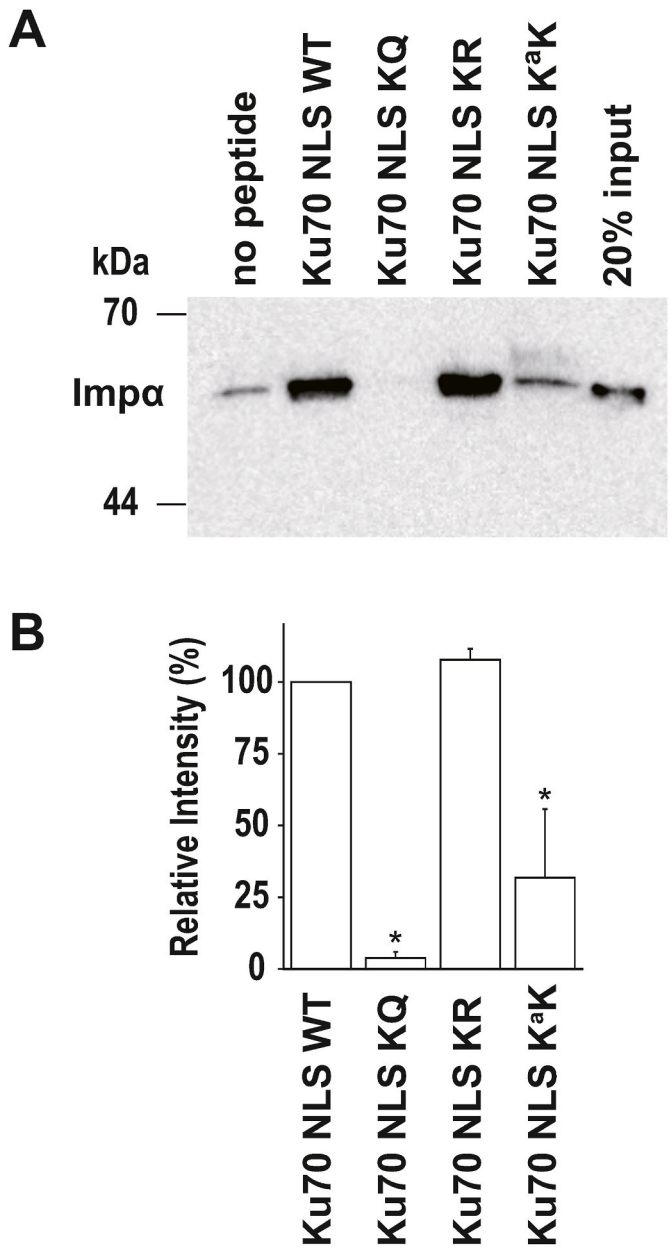

Fig. 1. Effect of substitution of lysine residues in the Ku70 NLS with acetyl–lysine on binding to Impα. **(A)** The effect of amino acid substitutions in the Ku70 NLS on Impα binding. The binding activity of Ku70 NLS and its mutant peptides to Impα in the presence of Impβ was analyzed by probing immunoblots with antibodies against Impα. **(B)** Quantification of the pull-down assays presented in panel **(A)**. Measurements of the blot band intensity were performed using ImageJ 1.52a. Each graph represents the relative intensity with Ku70 NLS WT defined as 100%. The error bars indicate the standard deviation from three independent experiments. *$p < 0.05$ significant differences from the case when the expected value was defined as 100.

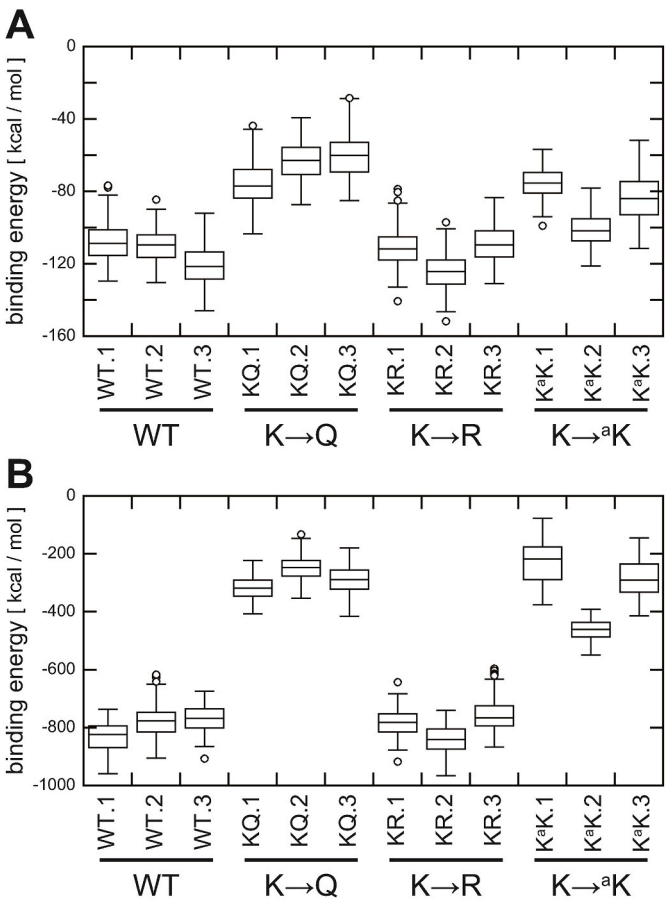

Fig. 2. Box plots of the distribution of binding energy between Impα and the Ku70 NLS during the simulation time. **(A)** Total binding energy (ΔG_{btot}) in solution and **(B)** total gas-phase energy (ΔG_{gas}) of Impα and wild-type Ku70 NLS (WT.1–WT.3), KQ mutants (KQ.1–KQ.3), KR mutants (KR.1–KR.3), or K^aK mutants ($K^aK.1$–$K^aK.3$) of Ku70 NLS. Note that lower binding energies indicate stronger interactions. Boxes represent half the amount of data in each respective distribution. The bars in each box indicate the median of the distribution. Open circles represent outlying data.

2. Materials and methods

2.1. Binding assay

Immobilization of the synthetic Ku70 NLS peptides (Eurofins Genomics, Tokyo, Japan) (Table S1) to Thiopropyl-Sepharose 6B (Sigma-Aldrich, St. Luis, MO, USA) was performed batchwise in a coupling buffer (0.1 M Tris–HCl, pH 7.5, 0.1 M NaCl, 1 mM EDTA) at room temperature (23 °C–25 °C) for 2 h. One mg of each peptide was used with 0.2 ml of swollen sepharose. After immobilization, the gel was treated with 5 mM dithiothreitol to remove the remaining 2-thiopyridyl groups on sepharose beads before washing with transport buffer (20 mM 4-(2-hydroxyethyl)-1-piperazineethanesulfonic acid, pH 7.3, 110 mM potassium acetate, 2 mM magnesium acetate, 5 mM sodium acetate, 1 mM ethylene glycol-bis(β-aminoethyl ether)-N,N,N′,N’-tetraacetic acid). A binding assay was performed with 50 μl NLS-immobilized sepharose, 1 mg/ml bovine serum albumin, 0.1 μg recombinant human Impα2 (NBP1-78888; Novus Biologicals, Centennial, CO, USA), and 0.1 μg recombinant human Impβ (NBP1-78815; Novus Biologicals) in 0.5 ml transport buffer by incubation for 2 h at 4 °C with gentle rotation. The gel was washed with transport buffer, and the bound importin was then eluted with sodium dodecyl sulfate–lysis buffer. The lysate was subjected to western blot analysis to detect Impα using an ImageQuant LAS 4000 (GE Healthcare, Chicago, IL, USA).

2.2. Molecular modeling and simulations

Molecular models of the wild-type or mutant Ku70 NLS in complex with Impα were constructed based on the reported crystallographic structure (PDB ID: 3RZX) [14], and 5-ns molecular dynamics (MD) simulations were executed. The binding free energies between the C-terminal region of the Ku70 NLS (N547 to E558) and its interaction site of Impα were calculated using coordinate sets obtained from each MD simulation by modifying the previous method [16]. The details are

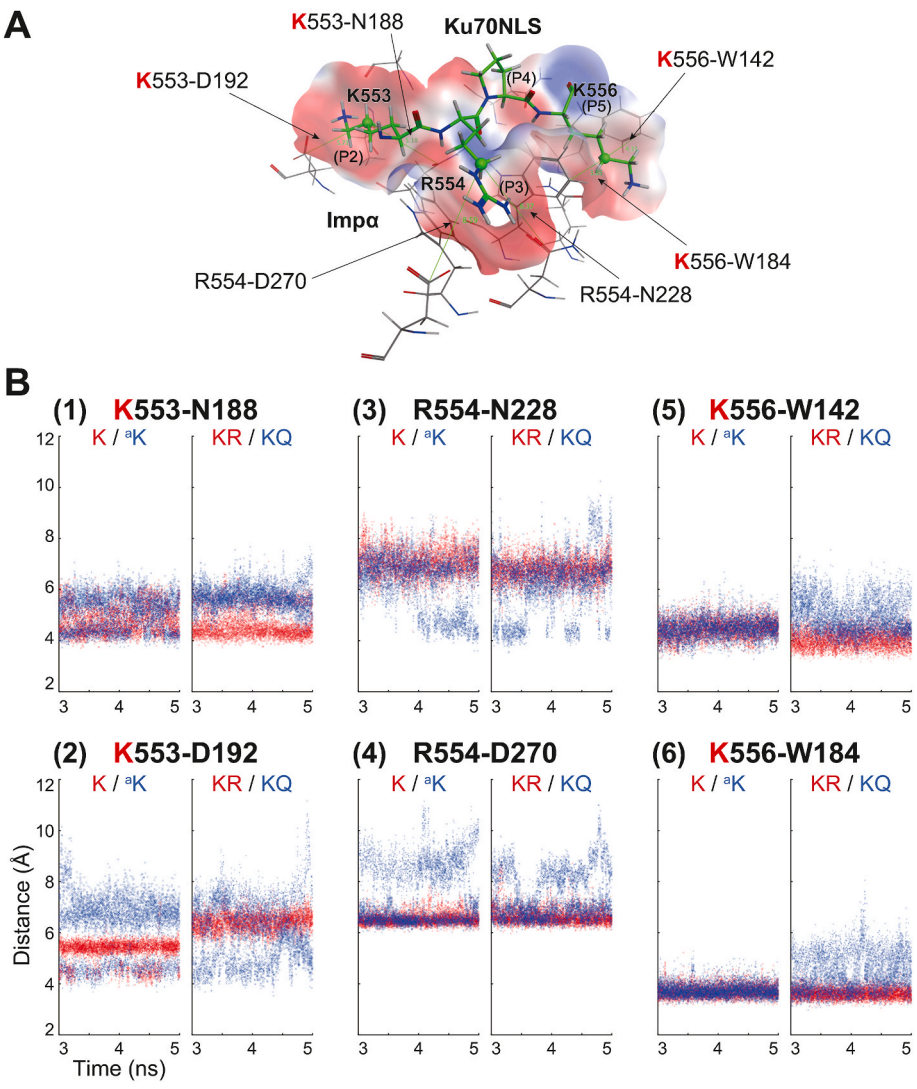

Fig. 3. Distances from a conserved residue in the contact site of the Ku70 NLS to adjacent residues in Impα during the simulation time. **(A)** Snapshot of the interaction site between Ku70 NLS and Impα. ^{553}KRPK^{556} of Ku70 NLS is illustrated as a green stick, and amino acids of Impα located near four Ku70 residues are presented as a gray stick. The molecular surface of Impα near the four Ku70 residues is also shown, with blue or red coloration on the surface indicating positive or negative charge, respectively. Pockets on the molecular surface in the major binding site of Impα are labeled as (P2) to (P5) [29]. **(B)** Distances between CD atoms in K553 of Ku70 and CG atoms in N188 and D192 of Impα ((1), (2)), CD atoms in R554 of Ku70, and CG atoms in N228 and D270 of Impα ((3), (4)), and CD atoms in K556 and CZ3 atoms in W142 and W184 of Impα ((5), (6)) are plotted during the simulation time from 3 to 5 ns (CD atoms in K553, R554, and K556 of the Ku70 NLS are represented as green balls in panel **(A)**). In each panel, the left graph represents the distribution of distances when none of the acetylation targets in the Ku70 NLS were replaced (K; red dots) or when they were replaced with acetyl–lysine (^{a}K; blue dots) residues, and the right graph indicates the distribution of distances when all acetylation targets in the Ku70 NLS were replaced with arginine (R; red dots) or glutamine (Q; blue dots) residues. (For interpretation of the references to color in this figure legend, the reader is referred to the Web version of this article.)

given in the supporting information.

2.3. Plasmid construction, cell lines, and transfection

cDNAs for human Ku70 were derived from pEGFP-Ku70 (1–609) [9,11]. Ku70 site-specific mutants were generated by incorporating mutant oligonucleotides via strand extension reactions, as previously described [11,17]. Following the application of the mutagenesis strategy, each mutant was identified by DNA sequencing. Chinese hamster xrs-6 cells defective in Ku80 (derived from CHO-K1 cells based on their sensitivity to ionizing radiation) were cultured [18,19]. Cells were transfected using FuGene6 (Roche Diagnostics, Indianapolis, IN, USA) or Lipofectamine 3000 (Invitrogen, Carlsbad, CA, USA).

3. Results

3.1. Substitution of Ku70 nuclear localization signal lysine residues to acetyl–lysine diminishes its interaction with importin-α/importin-β

Amino acid sequences in the Ku70 NLS region are well-conserved among primates. In particular, four of five lysine residues (K539, K542, K553, and K556) in human Ku70 are highly conserved among mammalian and avian Ku70 homologues, although K544 is replaced with a similar basic residue, arginine, in canine species [9,20] (Fig. S1).

A pull-down assay was performed to investigate whether the acetylation of lysine residues in the Ku70 NLS affects the interaction between Ku70 and the nuclear transport factors, Impα/Impβ (Fig. 1, Table S1). The peptide in which four lysine residues in the Ku70 NLS except K544 substituted with acetyl–lysine had a lower interaction with Impα/Impβ than the wild-type Ku70 NLS (Ku70 NLS WT and Ku70 NLS K^{a}K in Fig. 1). The effect of amino-acid substitutions with a charge-conservative residue, arginine, or with an uncharged residue, glutamine, for the same four lysine residues in the Ku70 NLS peptide was examined for later analyses. The peptide in which these lysine residues in the Ku70 NLS were substituted with arginine retained a high affinity for Impα in the presence of Impβ (Ku70 NLS KR in Fig. 1), and the substitution of the Ku70 NLS lysine residues to glutamine significantly diminished its interaction with Impα/Impβ (Ku70 NLS KQ in Fig. 1).

3.2. Structural analysis of the interaction site between the Ku70 nuclear localization signal and importin-α using molecular simulations

To analyze the molecular structure of the interaction site between the Ku70 NLS and Impα in detail, molecular models of the wild-type or mutant Ku70 NLS in complex with Impα were constructed, and 5-ns MD simulations were then conducted. Because the root mean square deviation values of all of the simulated molecules reached stable conditions after 3 ns of the MD simulation with few structural changes occurring (Fig. S2), distributions of the total binding energy (ΔG_{btot}) and total gas phase energy (ΔG_{gas}) between the Ku70 NLS and Impα were calculated

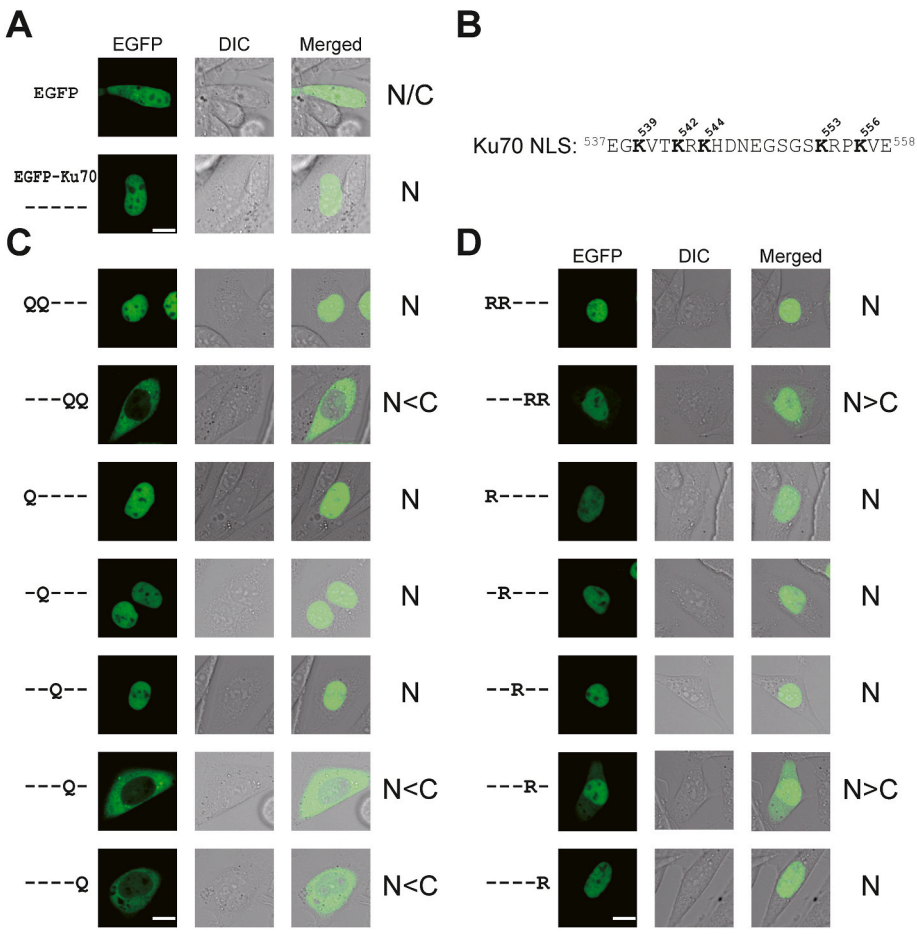

Fig. 4. Nuclear localization activity of Ku70. **(A)** EGFP signal, differential interference contrast (DIC), and merged images of the EGFP–wild-type Ku70 fusion protein and EGFP only in xrs-6 cells. Note that EGFP alone was localized throughout the cell owing to its having a small molecular mass, which allows its entry into the nucleus by passive diffusion [11]. **(B)** The amino acid sequence of the Ku70 NLS. Five lysine (K) residues that were reported as targets of acetylation are indicated in bold letters. Ku70 residue locations are indicated by numbers on either side of the sequence and above the lysine residues. **(C), (D)** KQ and KR mutant EGFP signals in xrs-6 cells. In **(A)**, **(C)**, and **(D)**, positions of substitution among the five lysine residues are indicated to the left of each panel; for example, "Q——" indicates a single mutation, K539Q. The predominance of localization in xrs-6 cells exhibiting translocation of the EGFP signal in each case is indicated to the right (N: nucleus, C: cytoplasm). The scale bar indicates 10 μm.

from the latter 2 ns of 5-ns MD simulation data (Fig. 2). The ΔG_{gas} term principally consists of electrostatic energy, excluding the contribution of solvation effects of the simulated system, and thus, it is strongly influenced by the total charge of amino acids in the contact region between the Ku70 NLS and Impα. In all three trials, the total gas phase energy between the Ku70 NLS and Impα was markedly suppressed when all lysine residues of interest were substituted with glutamine (K→Q in Fig. 2B), whereas they remained at the same level as that of the wild type when lysine residues were substituted with arginine (K→R in Fig. 2B). This order of binding energy in the gas phase was maintained even when solvation effects were considered (Fig. 2A). When the lysine residues of interest were replaced with acetyl–lysine residues (^{a}K), the binding energy in the gas phase decreased to the same level as that of KQ substitutions (K→^{a}K in Fig. 2B) and, in solution, approximately to the middle level between the wild-type and KR substitution mutants (K→^{a}K in Fig. 2A). These findings correspond with the results from the pull-down assay (Fig. 1) and imply that KQ or KR substitution mutants in the Ku70 NLS employ as a structural mimetic of acetylated lysine or non-acetylated [deacetylated] lysine.

The local movements of Ku70 NLS amino acid side chains in the binding sites on the molecular surface of Impα were studied to determine the stability of the Ku70 NLS–Impα complex (Fig. 3). The side chains of K553, R554, and K556 in the wild-type Ku70 NLS and R553, R554, and R556 in the KR mutant fitted into each contact pocket of Impα during the simulation time from 3 to 5 ns, with few changes occurring in the relative position between residues in the Ku70 NLS and their adjacent residues in Impα [red dots on the left and right graphs in Fig. 3B (1)–(6)]. In contrast, the conformation of the side chains of Q553, R554, and Q556 in the KQ mutant varied and did not remain constant in the contact pockets of Impα [blue dots in the right graphs in Fig. 3B (1)–(6)]. When K553 and K556 were replaced with acetylated lysine residues, the side chains of ^{a}K553 and R554 fluctuated widely as in the case of the KQ mutant [blue dots on the left graphs in Fig. 3B (1)–(4)], but the side chain movement of ^{a}K556 in the contact pocket of Impα remained the same as in the wild-type or KR mutant [blue dots on the left graphs in Fig. 3B (5) and (6)]. These findings indicate that ^{a}K556 continues to interact with its adjacent residues in Impα, and thus, this could be the reason why the Ku70 NLS with a K^{a}K substitution would have a slightly stronger interaction with Impα than the KQ mutant (Ku70 NLS K^{a}K in Fig. 1 and K→^{a}K in Fig. 2A).

3.3. *Mutations of lysine residues 553 and 556 inhibit the nuclear localization of Ku70*

We next attempted to obtain evidence that acetylation of lysine residues in the Ku70 NLS diminishes the nuclear localization of Ku70. However, it was technically infeasible to introduce an acetyl–lysine residue to a specific position in the full-size Ku70. Thus, we tested the nuclear translocation capacity of Ku70 mutants in which lysine residues in the NLS were replaced with glutamine residues as a putative structural imitation of acetylated lysine or with arginine as a structural mimetic of deacetylated lysine [21,22] (Fig. 4). For monitoring subcellular distribution in intact cells, the full-size Ku70 and its mutants were tagged with the fluorescent protein EGFP. We used endogenous Ku80-defective Chinese hamster ovary xrs-6 cells [18] as the parental cells in this investigation to explore the effects of amino acid changes on the nuclear translocation of Ku70 without the probable involvement of Ku80, which forms a heterodimer with Ku70. The double mutant EGFP-Ku70 K553Q/K556Q (—QQ in Fig. 4C) was detected mostly in the cytoplasm, but the double mutant EGFP-Ku70 K539Q/K542Q (QQ— in

Fig. 4C) was detected primarily in the nucleus. These results suggest that inhibition of the translocation of Ku70 from the cytoplasm to the nucleus is greater when a substituted lysine residue is located closer to the C-terminus of the Ku70 NLS. Single mutations at each acetylation site support this presumption. EGFP-Ku70 K553Q (—Q- in Fig. 4C) or EGFP-Ku70 K556Q (——Q in Fig. 4C) was detected primarily in the cytoplasm, whereas the wild-type Ku70 fusion proteins EGFP-Ku70 (——— in Fig. 4A), EGFP-Ku70 K539Q (Q—— in Fig. 4C), EGFP-Ku70 K542Q (-Q— in Fig. 4C) or EGFP-Ku70 K544Q (–Q– in Fig. 4C) were detected primarily in the nucleus, suggesting that two of the five lysine residues in the Ku70 NLS (K553 and K556) play more important roles in nuclear import of Ku70. In contrast, the inhibition of Ku70 translocation to the nucleus was not significant when K539, K542, K544, or K556 was replaced separately or when K539/K542 was substituted concurrently with arginine residues (RR—, R——, -R—, –R–, ——R in Fig. 4D). The level of nuclear localization of Ku70 was declined slightly when K553 was replaced with arginine (—RR, —R- in Fig. 4D). These observations are consistent with the consequence deduced from several preceding studies that the first amino acid in the typical NLS motif (K553 of ^{553}KRPK^{556} in the case of the Ku70 NLS) should be a lysine [23–25].

4. Discussion

The molecular structures of the core of the Ku heterodimer and the C-terminal DNA-binding domain (SAP domain) of Ku70 were separately resolved by X-ray crystallographic and nuclear magnetic resonance analysis, respectively [26,27]. The Ku70 NLS is found in the linker region that connects these two parts of Ku70 and is assumed to be unable to fold into a specific three-dimensional structure on its own. It was reported that at least eight lysine residues in Ku70 are targets for acetylation [6] and five of those eight lysine residues are concentrated in the linker region. In solution, this disordered region is likely flexible and long enough for regulatory proteins such as Impα to bind with Ku70 without sterically interfering with the remainder of the Ku70 molecule (Fig. S3).

In the current study, two of five lysine residues in the C-terminus of the Ku70 NLS, K553 and K556, were identified as strong candidates for modulating the nuclear transport of Ku70 (Fig. 4), although the remaining three lysine residues were also found to contribute to the nuclear transport function in the previous study [9]. Interestingly, the substitution of either K539 or K542 with glutamine abolished the binding of cytosolic Ku70 to both Bax and FLIP [6,7,28]. As a result, acetylation of the five lysine residues in the Ku70 NLS appears to have bifunctional biological consequences: acetylation of K553 and K556 suppresses Ku70 nuclear transport for DSB repair, whereas acetylation of K539 or K542 appears to facilitate activation of the two apoptosis pathways, though the biological significance of acetylation of K544 in the Ku70 NLS remains unknown. Further structural analyses are required to clarify this.

Declaration of competing interest

The authors declare that they have no known competing financial interests or personal relationships that could have appeared to influence the work reported in this paper.

Acknowledgments

The authors would like to thank Prof. P. Jeggo for providing xrs-6 cells and Dr. H. Ode for preparing the computer script to assemble MM/PBSA data. We also thank Dr. K. Hanada for carefully proofreading the manuscript and Enago (www.enago.jp) for the English language review. This work was supported in part by JSPS KAKENHI (grant number: 19K12337).

Appendix A. Supplementary data

Supplementary data to this article can be found online at https://doi.org/10.1016/j.bbrep.2022.101418.

References

[1] D.B. Swartzlander, N.C. Bauer, A.H. Corbett, P.W. Doetsch, Regulation of base excision repair in eukaryotes by dynamic localization strategies, Prog. Mol. Biol. Transl. Sci. 110 (2012) 93–121, https://doi.org/10.1016/B978-0-12-387665-2.00005-5.
[2] N.C. Bauer, P.W. Doetsch, A.H. Corbett, Mechanisms regulating protein localization, Traffic 16 (2015) 1039–1061, https://doi.org/10.1111/tra.12310.
[3] B.L. Mahaney, K. Meek, S.P. Lees-Miller, Repair of ionizing radiation-induced DNA double-strand breaks by non-homologous end-joining, Biochem. J. 417 (2009) 639–650, https://doi.org/10.1042/BJ20080413.
[4] M. Koike, Y. Yutoku, A. Koike, Accumulation of Ku70 at DNA double-strand breaks in living epithelial cells, Exp. Cell Res. 317 (2011) 2429–2437, https://doi.org/10.1016/j.yexcr.2011.07.018.
[5] M. Koike, T. Awaji, M. Kataoka, G. Tsujimoto, T. Kartasova, A. Koike, T. Shiomi, Differential subcellular localization of DNA-dependent protein kinase components Ku and DNA-PKcs during mitosis, J. Cell Sci. 112 (1999) 4031–4039, https://doi.org/10.1242/jcs.112.22.4031.
[6] H.Y. Cohen, S. Lavu, K.J. Bitterman, B. Hekking, T.A. Imahiyerobo, C. Miller, R. Frye, H. Ploegh, B.M. Kessler, D.A. Sinclair, Acetylation of the C terminus of Ku70 by CBP and PCAF controls Bax-mediated apoptosis, Mol. Cell. 13 (2004) 627–638, https://doi.org/10.1016/S1097-2765(04)00094-2.
[7] E. Kerr, C. Holohan, K.M. McLaughlin, J. Majkut, S. Dolan, K. Redmond, J. Riley, K. McLaughlin, I. Stasik, M. Crudden, S. Van Schaeybroeck, C. Fenning, R. O'Connor, P. Kiely, M. Sgobba, D. Haigh, P.G. Johnston, D.B. Longley, Identification of an acetylation-dependant Ku70/FLIP complex that regulates FLIP expression and HDAC inhibitor-induced apoptosis, Cell Death Differ. 19 (2012) 1317–1327, https://doi.org/10.1038/cdd.2012.8.
[8] S. Mazumder, D. Plesca, M. Kinter, A. Almasan, Interaction of a cyclin E fragment with Ku70 regulates Bax-mediated apoptosis, Mol. Cell Biol. 27 (2007) 3511–3520, https://doi.org/10.1128/MCB.01448-06.
[9] M. Koike, T. Ikuta, T. Miyasaka, T. Shiomi, The nuclear localization signal of the human Ku70 is a variant bipartite type recognized by the two components of nuclear pore-targeting complex, Exp. Cell Res. 250 (1999) 401–413, https://doi.org/10.1006/excr.1999.4507.
[10] M. Koike, T. Shiomi, A. Koike, Ku70 can translocate to the nucleus independent of Ku80 translocation and DNA-PK autophosphorylation, Biochem. Biophys. Res. Commun. 276 (2000) 1105–1111, https://doi.org/10.1006/bbrc.2000.3567.
[11] M. Koike, T. Shiomi, A. Koike, Dimerization and nuclear localization of Ku proteins, J. Biol. Chem. 276 (2001) 11167–11173, https://doi.org/10.1074/jbc.M010902200.
[12] M. Koike, Dimerization, translocation and localization of Ku70 and Ku80 proteins, J. Radiat. Res. 43 (2002) 223–236, https://doi.org/10.1269/jrr.43.223.
[13] G. Alvisi, L. Paolini, A. Contarini, C. Zambarda, V. Di Antonio, A. Colosini, N. Mercandelli, M. Timmoneri, G. Palu, L. Caimi, D. Ricotta, A. Radeghieri, Intersectin goes nuclear: secret life of an endocytic protein, Biochem. J. 475 (2018) 1455–1472, https://doi.org/10.1042/BCJ20170897.
[14] A.A. Takeda, A.C. de Barros, C.W. Chang, B. Kobe, M.R. Fontes, Structural basis of importin-alpha-mediated nuclear transport for Ku70 and Ku80, J. Mol. Biol. 412 (2011) 226–234, https://doi.org/10.1016/j.jmb.2011.07.038.
[15] X.J. Yang, E. Seto, Lysine acetylation: codified crosstalk with other posttranslational modifications, Mol. Cell. 31 (2008) 449–461, https://doi.org/10.1016/j.molcel.2008.07.002.
[16] H. Fujimoto, M. Higuchi, M. Koike, H. Ode, M. Pinak, J.K. Bunta, T. Nemoto, T. Sakudoh, N. Honda, H. Maekawa, K. Saito, K. Tsuchida, A possible overestimation of the effect of acetylation on lysine residues in KQ mutant analysis, J. Comput. Chem. 33 (2012) 239–246, https://doi.org/10.1002/jcc.21956.
[17] M. Koike, T. Ikuta, T. Miyasaka, T. Shiomi, Ku80 can translocate to the nucleus independent of the translocation of Ku70 using its own nuclear localization signal, Oncogene 18 (1999) 7495–7505, https://doi.org/10.1038/sj.onc.1203247.
[18] B.K. Singleton, A. Priestley, H. Steingrimsdottir, D. Gell, T. Blunt, S.P. Jackson, A. R. Lehmann, P.A. Jeggo, Molecular and biochemical characterization of xrs mutants defective in Ku80, Mol. Cell Biol. 17 (1997) 1264–1273, https://doi.org/10.1128/MCB.17.3.1264.
[19] M. Koike, A. Koike, The establishment and characterization of cell lines stably expressing human Ku80 tagged with enhanced green fluorescent protein, J. Radiat. Res. 45 (2004) 119–125, https://doi.org/10.1269/jrr.45.119.
[20] M. Koike, Y. Yutoku, A. Koike, Cloning, localization and focus formation at DNA damage sites of canine Ku70, J. Vet. Med. Sci. 79 (2017) 554–561, https://doi.org/10.1292/jvms.16-0649.
[21] S.C. Kim, R. Sprung, Y. Chen, Y. Xu, H. Ball, J. Pei, T. Cheng, Y. Kho, H. Xiao, L. Xiao, N.V. Grishin, M. White, X.J. Yang, Y. Zhao, Substrate and functional diversity of lysine acetylation revealed by a proteomics survey, Mol. Cell. 23 (2006) 607–618, https://doi.org/10.1016/j.molcel.2006.06.026.
[22] K. Kamieniarz, R. Schneider, Tools to tackle protein acetylation, Chem. Biol. 16 (2009) 1027–1029, https://doi.org/10.1016/j.chembiol.2009.10.002.
[23] M.R. Hodel, A.H. Corbett, A.E. Hodel, Dissection of a nuclear localization signal, J. Biol. Chem. 276 (2001) 1317–1325, https://doi.org/10.1074/jbc.M008522200.

[24] M.R. Fontes, T. Teh, D. Jans, R.I. Brinkworth, B. Kobe, Structural basis for the specificity of bipartite nuclear localization sequence binding by importin-alpha, J. Biol. Chem. 278 (2003) 27981–27987, https://doi.org/10.1074/jbc.M303275200.

[25] S. Kosugi, M. Hasebe, N. Matsumura, H. Takashima, E. Miyamoto-Sato, M. Tomita, H. Yanagawa, Six classes of nuclear localization signals specific to different binding grooves of importin alpha, J. Biol. Chem. 284 (2009) 478–485, https://doi.org/10.1074/jbc.M807017200.

[26] J.R. Walker, R.A. Corpina, J. Goldberg, Structure of the Ku heterodimer bound to DNA and its implications for double-strand break repair, Nature 412 (2001) 607–614, https://doi.org/10.1038/35088000.

[27] Z. Zhang, L. Zhu, D. Lin, F. Chen, D.J. Chen, Y. Chen, The three-dimensional structure of the C-terminal DNA-binding domain of human Ku70, J. Biol. Chem. 276 (2001) 38231–38236, https://doi.org/10.1074/jbc.M105238200.

[28] C. Subramanian, A.W. Opipari Jr., X. Bian, V.P. Castle, R.P. Kwok, Ku70 acetylation mediates neuroblastoma cell death induced by histone deacetylase inhibitors, Proc. Natl. Acad. Sci. U. S. A. 102 (2005) 4842–4847, https://doi.org/10.1073/pnas.0408351102.

[29] M.R. Hodel, A.H. Corbett, A.E. Hodel, Dissection of a nuclear localization signal, J. Biol. Chem. 276 (2001) 1317–1325, https://doi.org/10.1074/jbc.M008522200.